Leveraging iPSC-derived Astrocytes to Accelerate the Discovery of Novel **Drugs Targeting Neuroinflammation**

¹T. Modebadze, ¹M.Gurney, ¹H.Scott, ¹S.J. McCafferty, ¹M. Paterson, ²J.Sleight, ²D.Pearce, ³S.M. Walter, ³K. Keska-Izworska, ³L. Fillinger, ³M. Ley, ³P. Perco, ³K. Kratochwill, ¹E. Malavasi.

¹Concept Life Sciences, Edinburgh, United Kingdom, ²Fios Genomics, Edinburgh, United Kingdom, ³Delta4, Vienna, Austria.

CONCEPT LIFE SCIENCES





1. Introduction

Astrocytes, the most abundant glial population in the human central nervous system, normally play critical roles in neuroprotection, immunity, and homeostasis. However, upon exposure to specific neuroinflammatory cues, astrocytes assume a pro-inflammatory, neurotoxic phenotype. Neurotoxic astrocytes promote chronic neuroinflammation, a common driver of many neurodegenerative diseases. Thus, identifying and targeting the signalling pathways that lead to the formation of neurotoxic astrocytes can provide novel therapeutic approaches to curb neurodegeneration. The preclinical development of new drugs targeting neurotoxic astrocytes requires scalable, robust and reproducible assays that harness accurate, translational and accessible in vitro models of the neurotoxic phenotype. Here, we aimed to: i. Assess the validity of human iPSC-derived astrocytes exposed to neuroinflammatory stimuli as a representative model of neurotoxic reactive astrocytes (NRA); ii. Develop and validate an NRA polarisation assay and iii. Leverage our model and assay to identify new drug targets to inhibit or reverse the pro-inflammatory neurotoxic phenotype.

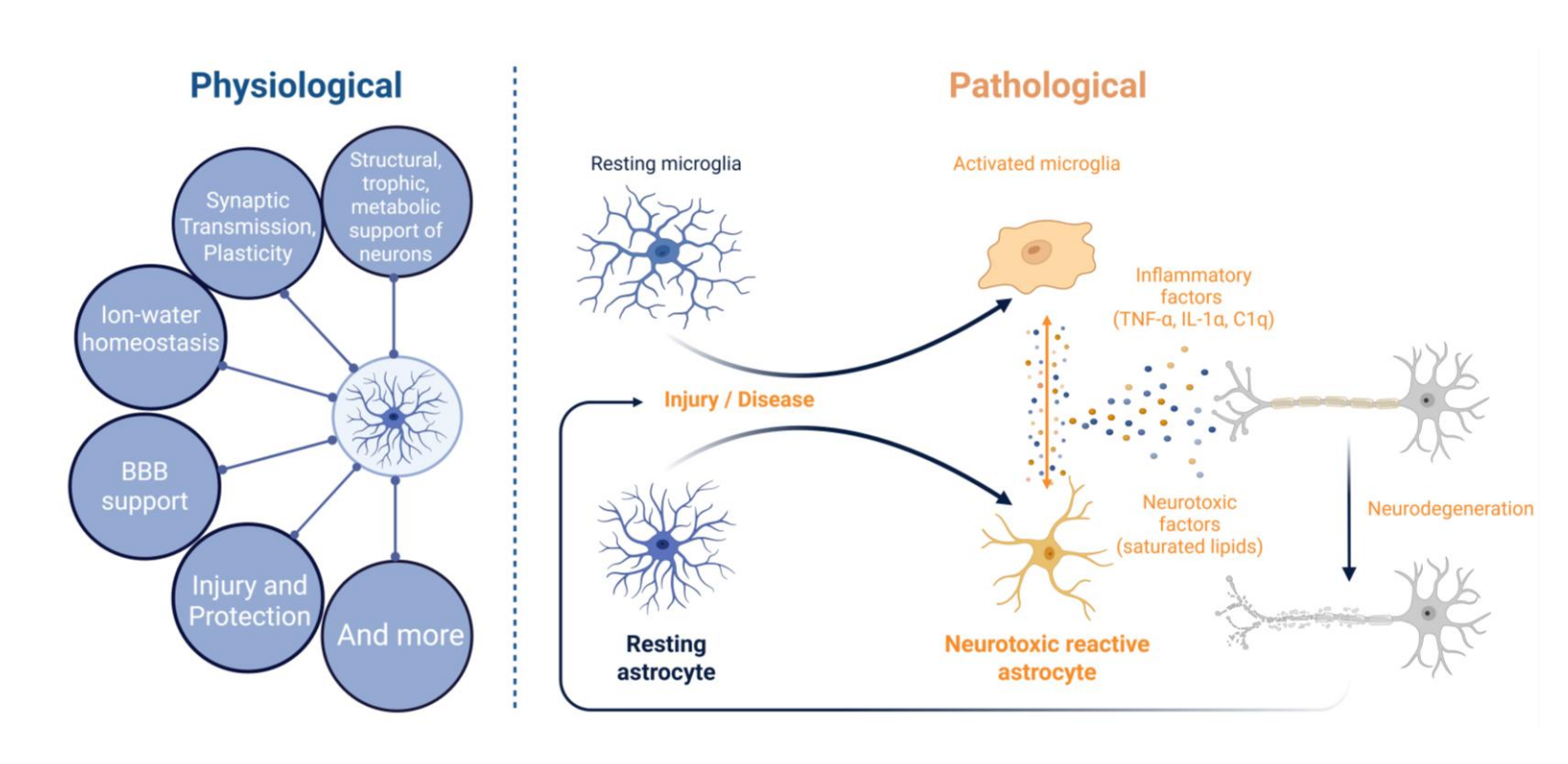


Figure 1: Astrocytes downregulate neuroprotective functions and acquire a neurotoxic phenotype in neurodegenerative diseases.

2. Methods (1) Astrocyte Polarization 24h TIC or PBS Lot Comparison Positive Control Validation Pre-differentiated

Figure 2: Pre-differentiated cryopreserved human iPSC-derived astrocytes from a single donor were cultured for 8 days. For bulk RNA sequencing (RNAseq), cells from two different lots were treated with TNF α , IL-1 α and C1q (TIC) or PBS for 24 hours. Cytokine secretion was assessed via Luminex on pooled supernatants. Cells were lysed and RNA extracted in triplicates for sequencing (~20 million paired end reads/sample). Differential gene expression analysis was performed in R. For positive control validation, astrocytes from two or three different lots were pre-treated with Dexamethasone (Dex) or vehicle (DMSO) for 1 hour, before TIC or PBS exposure for a further 24 hours. Cytokine secretion profile was assessed via Luminex, gene expression was analysed by qPCR.

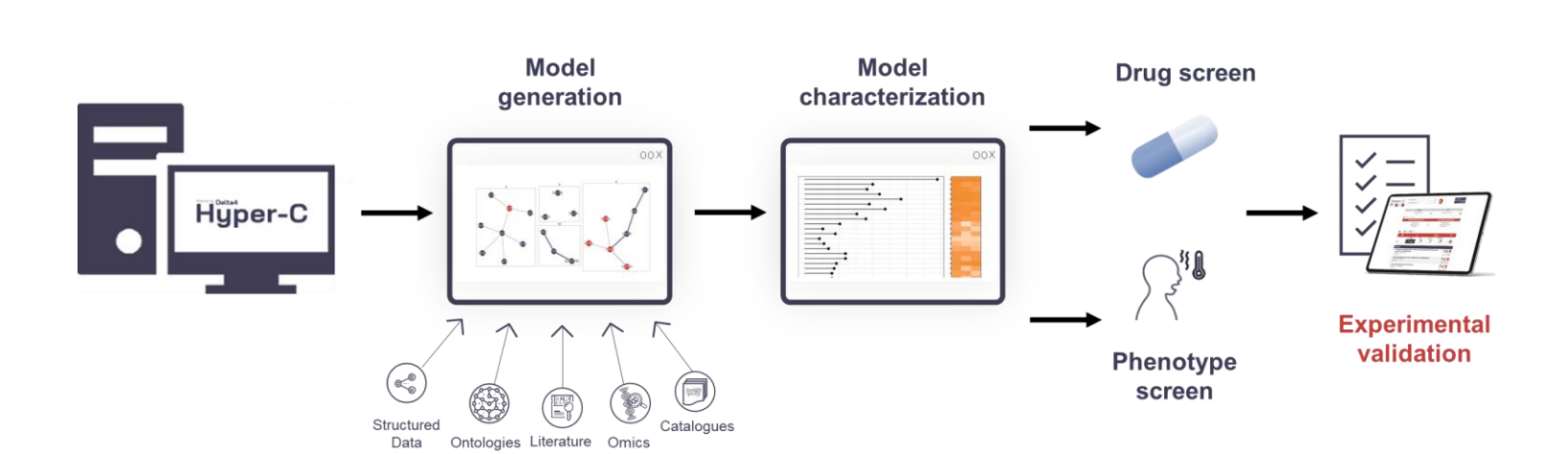


Figure 3: Computational astrocyte model generation and evaluation. We built a computational astrocyte model that integrates multiple data sources within the Delta4 knowledge graph (KG) Hyper-C. Core associations include genes linked to astrocytes and mechanisms such as 'astrocyte activation' and 'neuroinflammation' (275 genes). This core is expanded with i. Astrocyte-specific genes from the Human Protein Atlas (Tau > 0.9; 51 genes), ii. Differentially expressed genes strongly connected via the Hyper-C PPI network (156 genes), iii. Genes relevant to neurotoxic and neuroprotective astrocyte subsets from selected reviews (97 genes) (Cameron et al., Escartin et al., Lawrence et al.).

3. Baseline Transcriptional Profiling of iPSC-derived astrocytes

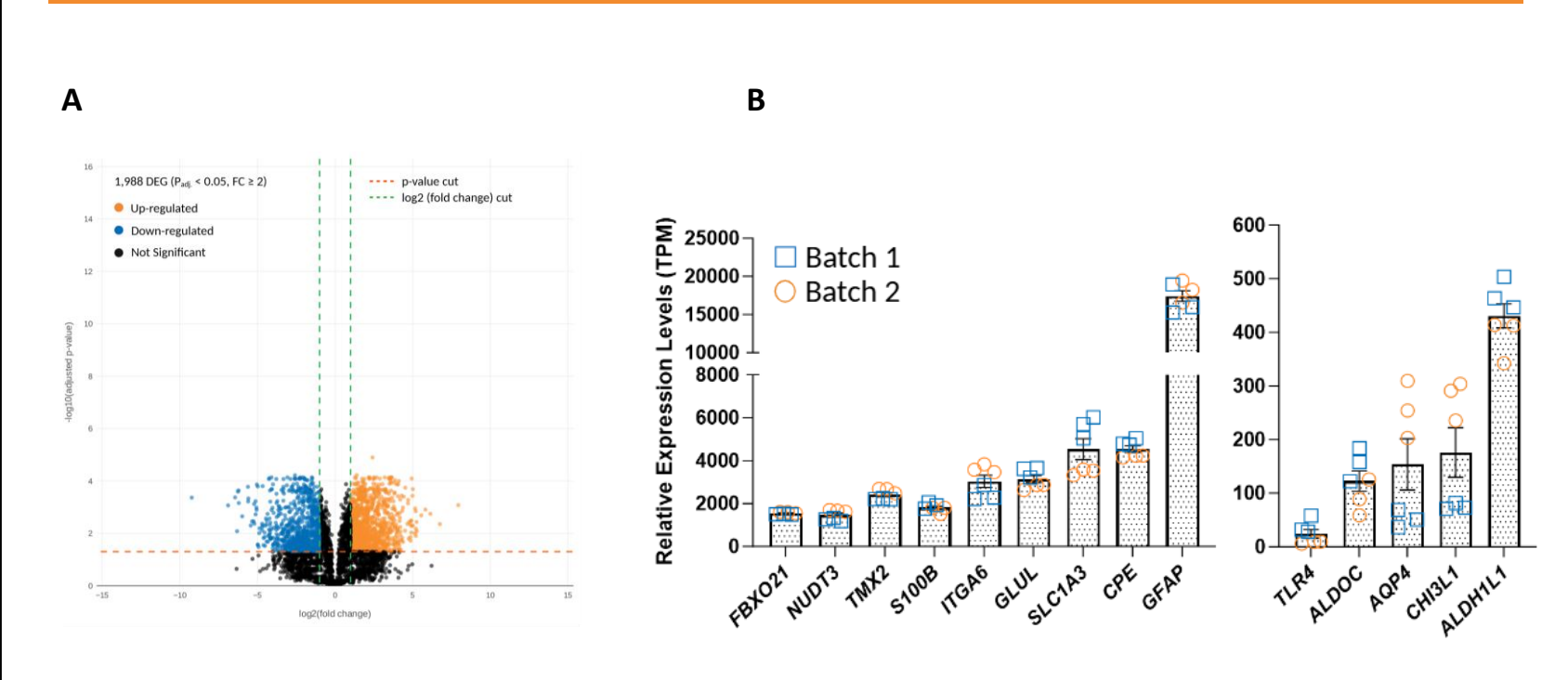
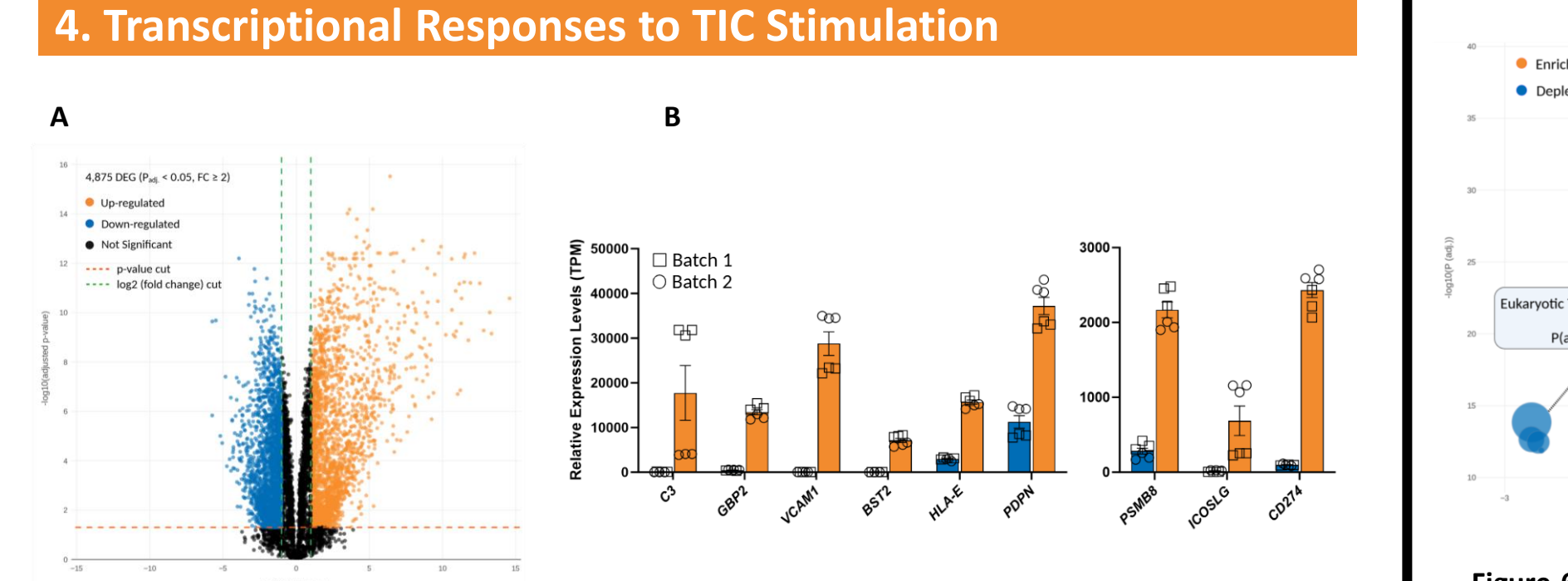
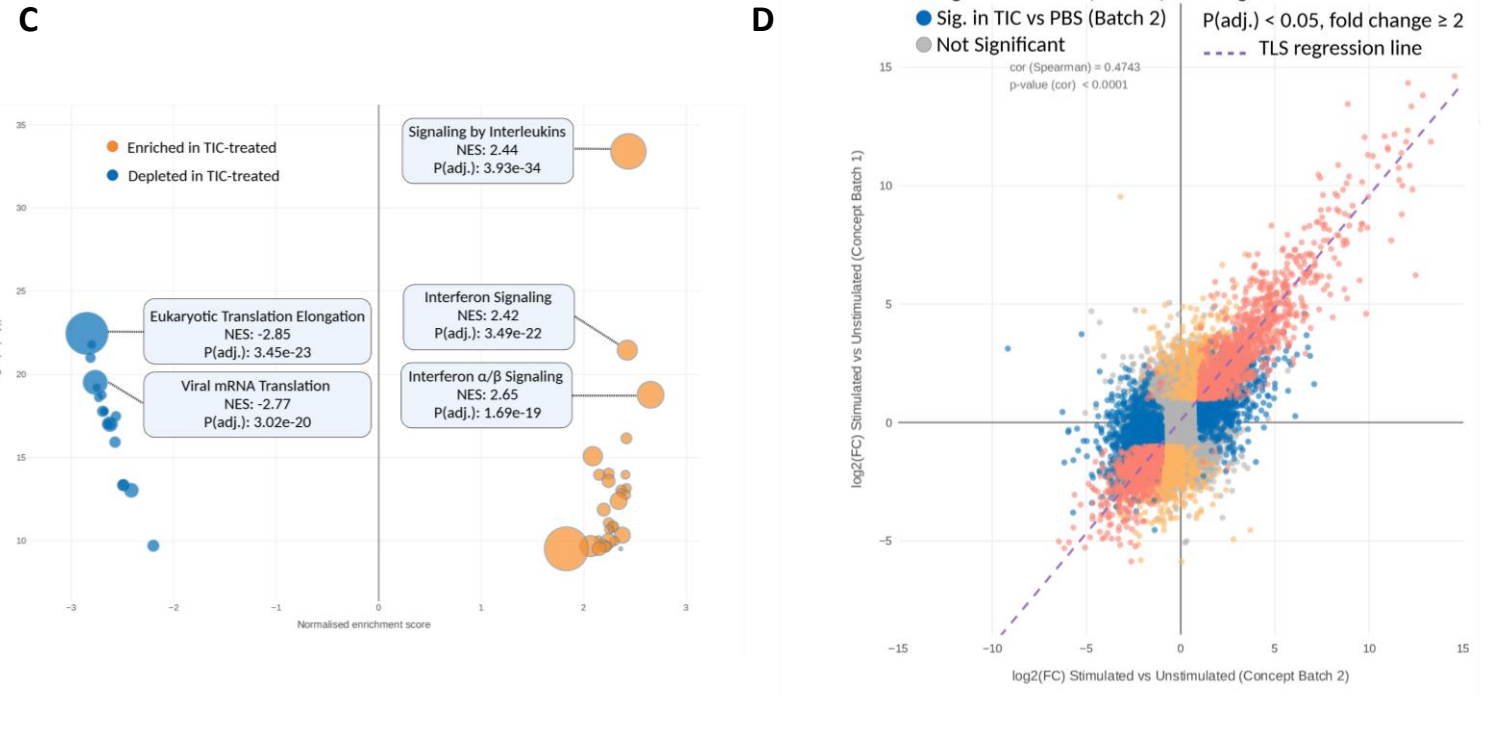


Figure 4: (A) Volcano plot showing upregulated and downregulated differentially expressed genes (DEG) in astrocytes from Batch 1 vs. Batch 2. (B) Transcript per million (TPM) expression levels of mature astrocyte markers in Batch 1 (blue) and Batch 2 (orange). Data is presented as mean ± SEM.



Sig. in TIC vs PBS (Batch 1)
Significant in both



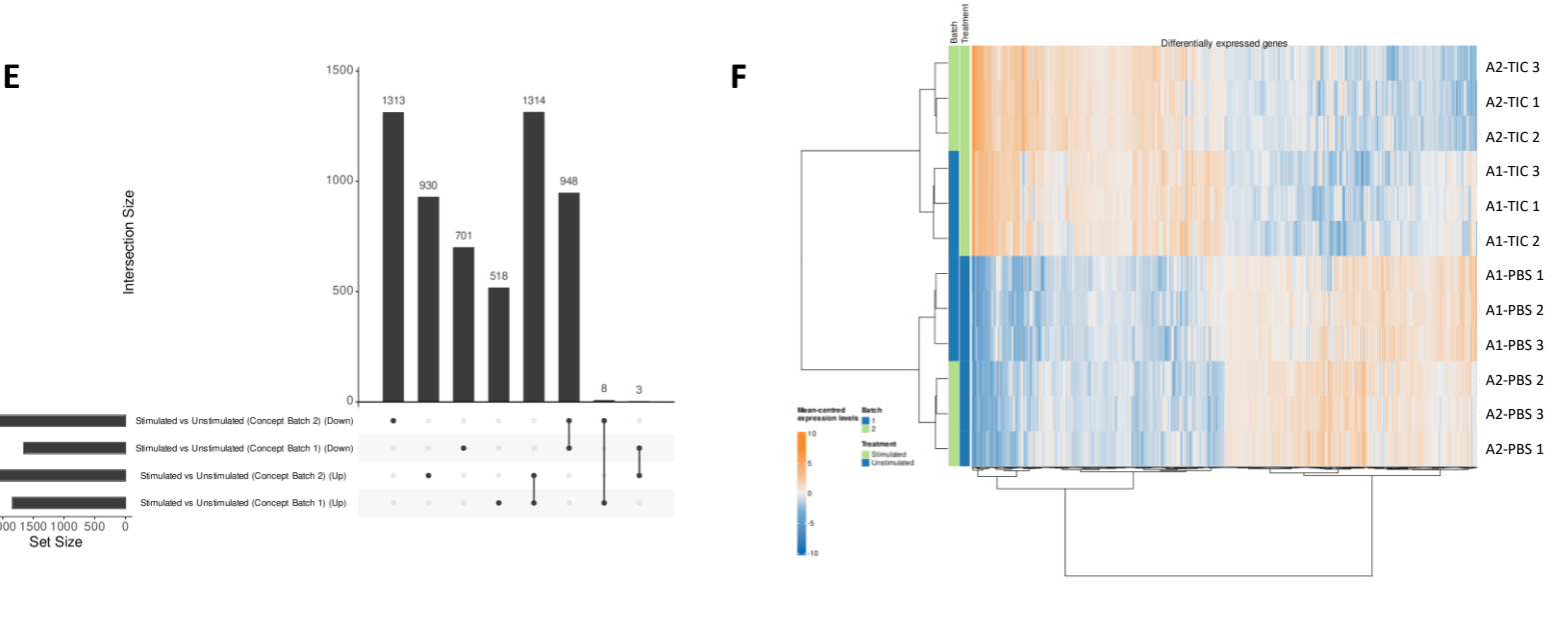
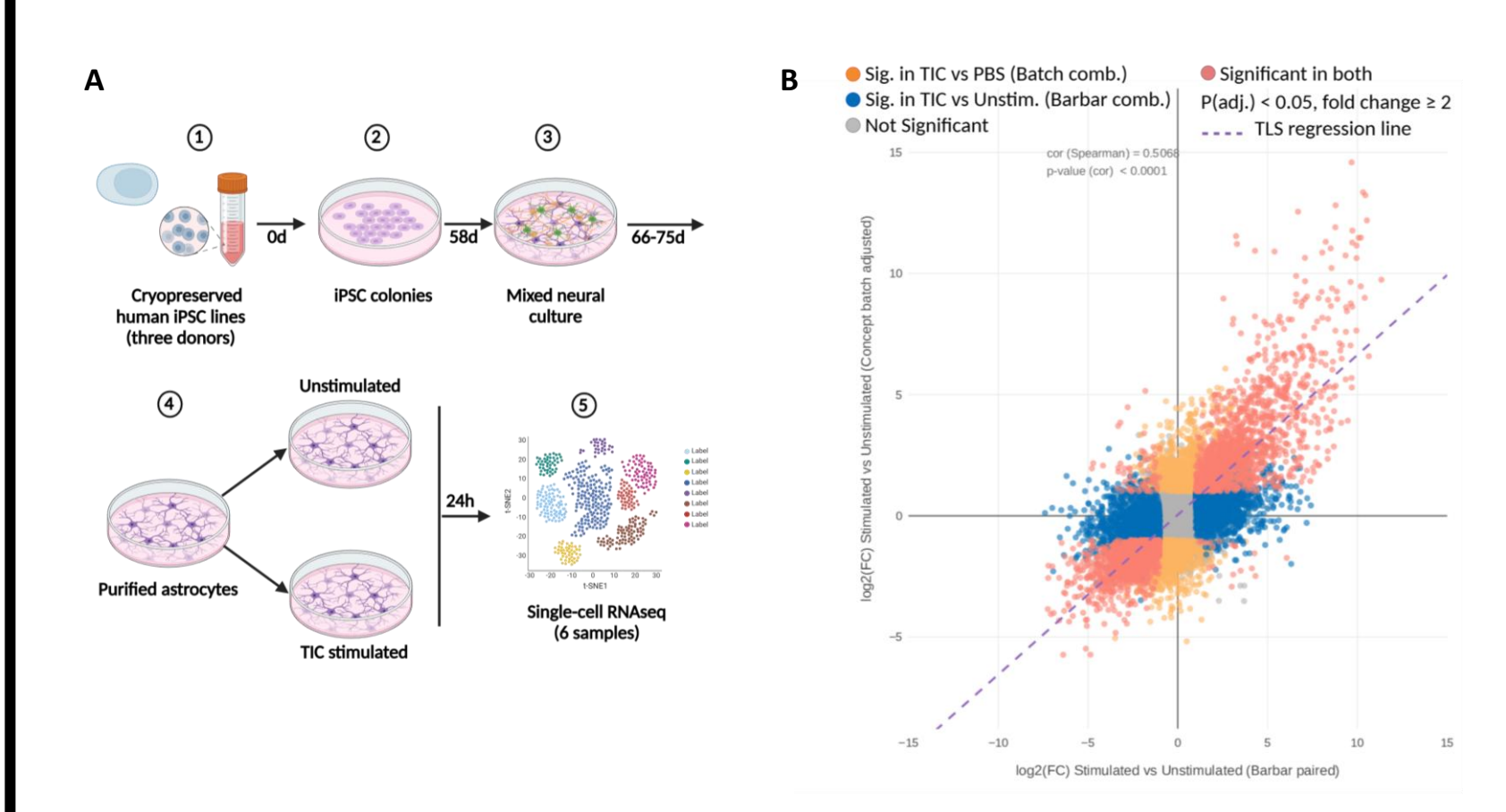


Figure 5: (A) Volcano plot showing upregulated and downregulated DEG in TIC-treated vs. PBS-treated astrocytes from Batches 1 and 2 combined. (B) TPM expression levels of known neurotoxic astrocyte markers in PBS-treated (blue) and TIC-treated (orange) astrocytes. Data is presented as mean \pm SEM. (C) Bubble plot of statistical significance of pathway-specific gene set enrichment (GSE) $-\log_{10}(adjusted)$ p-value) against normalized enrichment score in TIC-treated vs. PBS-treated astrocytes from Batches 1 and 2 combined. The size of each bubble reflects the number of genes evaluated for each pathway. (D) Congruence analysis comparing $log_2(FC)$ of significant genes in TIC-treated vs. PBS-treated astrocytes from Batch 1 vs. Batch 2. (E) Upset plot showing the interaction between sets of up- and downregulated genes in TIC-treated vs PBS-treated astrocytes from Batch 1 vs. Batch 2. The leftmost bar chart shows the size of each set used as input. The top bar chart shows the exclusive size of each set (i.e., each gene is only counted once in this bar chart). The dot-plot in the centre shows the sets interacting in each case. **(F)** Heatmap showing gene intensity per sample relative to the average level

5. Comparison to Publicly Available Transcriptomic Data



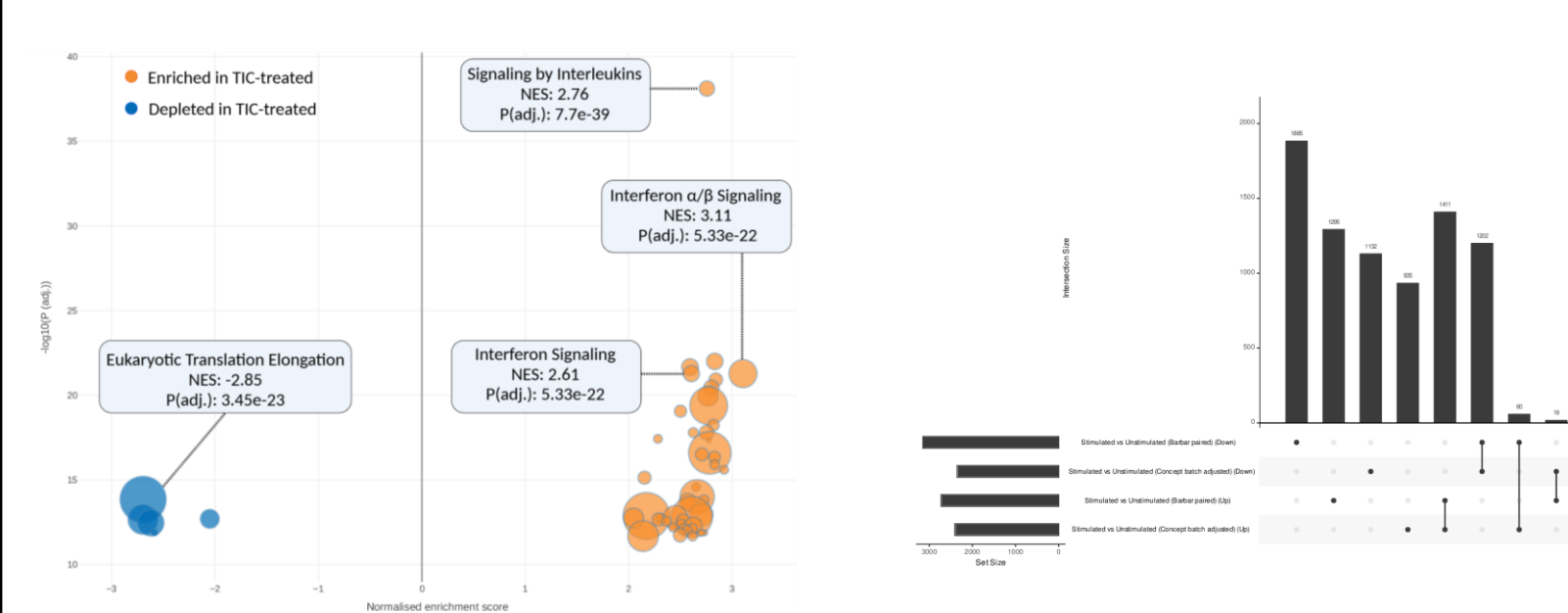


Figure 6: (A) Diagram summarising the experimental procedure described by Barbar et al. 2020. (B) Congruence analysis comparing log₂(FC) of significant genes in TIC-treated vs. PBS-treated astrocytes from Concept combined vs. Barbar combined datasets. (C) Upset plot showing the interaction between sets of up- and down-regulated genes in Concept combined vs. Barbar combined datasets (D) Bubble plot of statistical significance of pathway-specific GSE -log₁₀(adjusted p-value) against normalized enrichment score in the Barbar combined datasets. The size of each bubble reflects the number of genes evaluated for each pathway.

6. Positive Control Validation

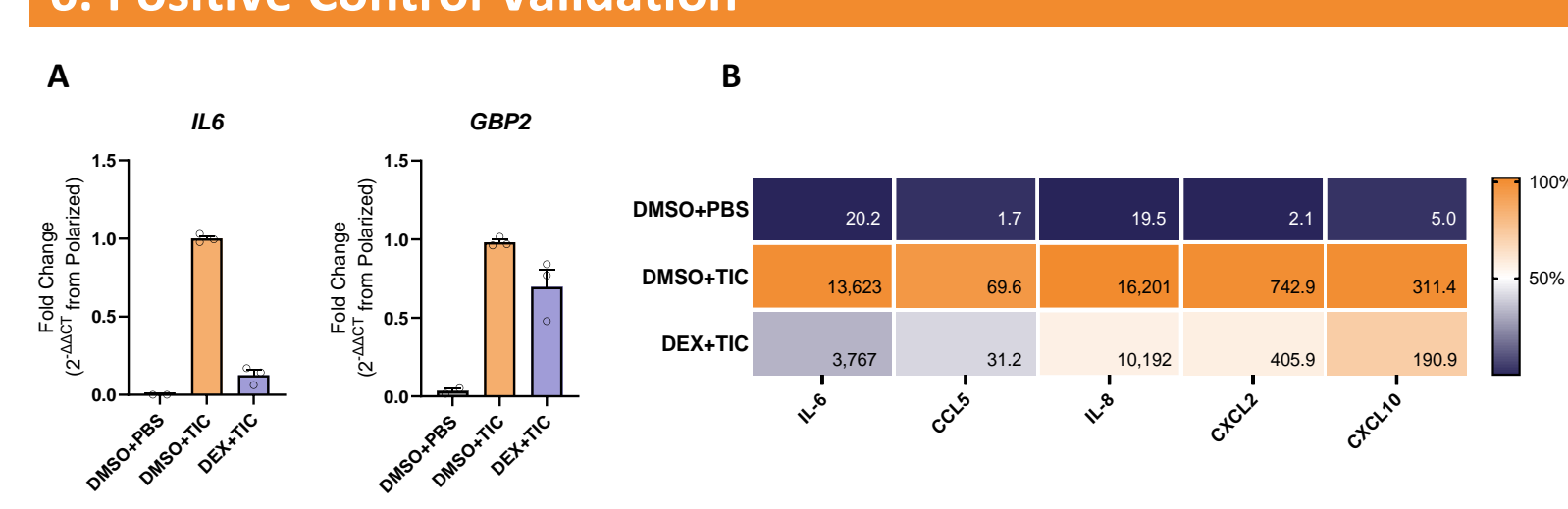


Figure 7: (A) Gene expression analysis in astrocytes pre-treated with Dex or vehicle and polarized with the TIC cocktail. Data presented as mean + SEM fold-change ($2^{-\Delta\Delta Ct}$) calculated relative to the DMSO + TIC control (n = 3 lots, 3 experimental repeats total, 3 qPCR technical replicates). (B) Heat map showing cytokine secretion profile in astrocytes pre-treated with Dex or vehicle and polarized with the TIC cocktail. The heatmap represents the median percentage of DMSO + TIC (n = 2 lots, 3 experimental repeats total, 5 technical replicates each). Values represent median concentrations

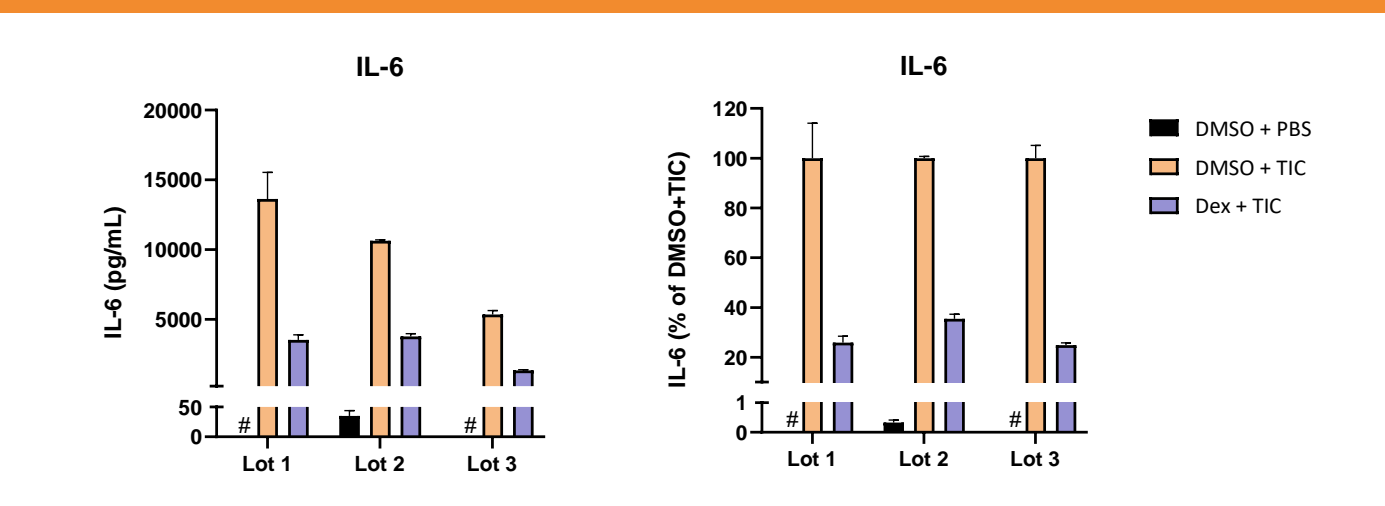


Figure 8: IL-6 secretion in astrocytes pre-treated with Dex or vehicle and polarized with the TIC cocktail. Data presented as mean + SEM concentration or percentage of polarized vehicle control (n = 3 lots, 3 experimental repeats total, 5 technical replicates). # denotes conditions where values were below detection.

8. Generation of a Computational Astrocyte Model

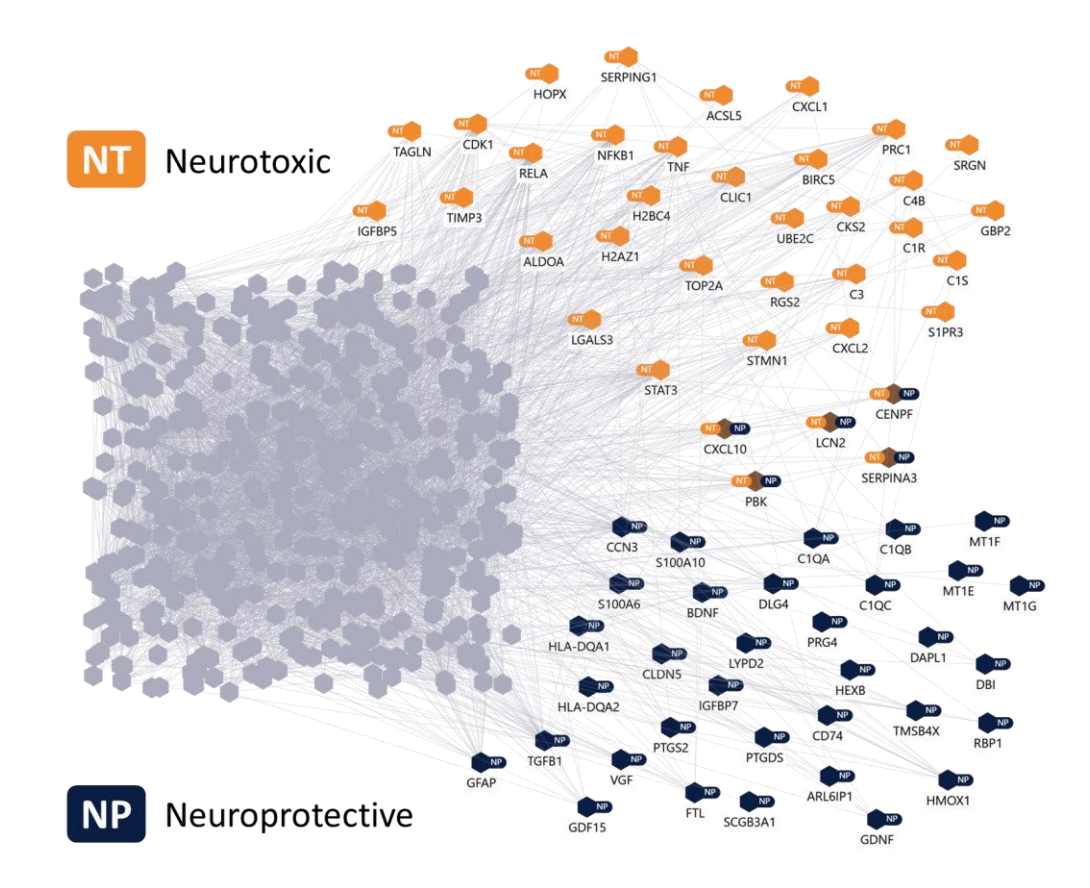


Figure 9: Astrocyte model. Astrocyte model with labelled subnetworks for neurotoxic (orange) and neuroprotective (blue) phenotypes. The model has a size of 522 genes. Edges are based on the Hyper-C PPI network.

9. Computational Drug Screening

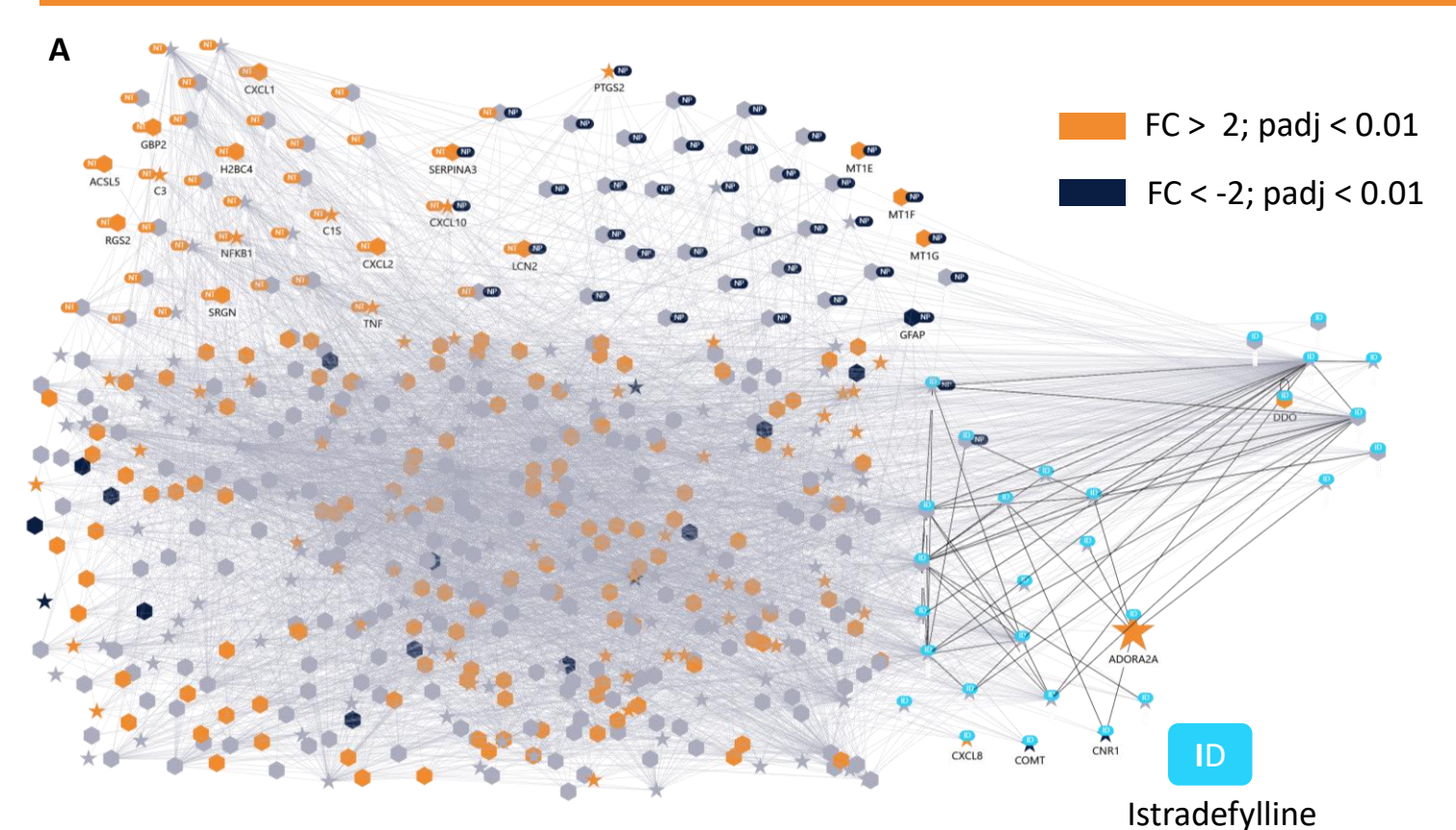
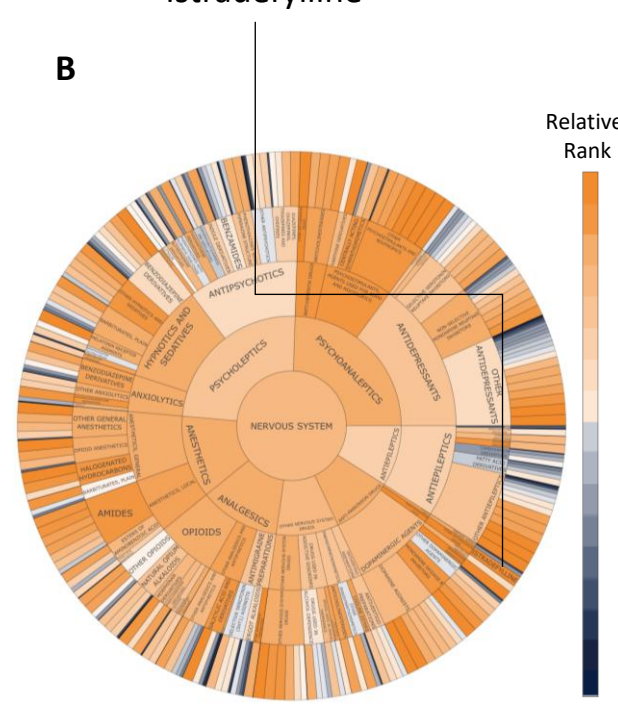


Figure 10: Astrocyte model with drug screening result. B Screening the Hyper-C drug library with the astrocyte model recovered the approved drug Istradefylline for Parkinson's Disease in the top 3% of all drugs (> 4000). Relative ranks for drugs in the nervous system are shown in (B). All drug targets in the astrocyte model are highlighted as 'stars' in (A), with the drug target of Istradefylline, ADORA2A, labelled additionally. Up- and downregulation from RNAseq is shown in orange and blue respectively and gene symbols are labelled for selected nodes. ADORA2A is an upregulated receptor in reactive astrocytes, while Istradefylline is a selective antagonist of the same receptor, which is also described in the literature to regulate microglial activation in late phases of inflammation (Ogawa et al, 30026035). Drug repositioning methodology follows Perco et al. 2025.



10. Conclusions

- Here we demonstrate the validity of pre-differentiated cryopreserved iPSC-derived astrocytes as a model to study neuroinflammatory responses. We have shown that these astrocytes:
- Express key markers of mature astrocytes and display a consistent batch-to-batch transcriptomic profile.
- Respond to TIC stimulation in a manner that is consistent with what observed in an independently generated iPSC-derived astrocyte population.
- Display robust TIC-driven induction of pro-inflammatory markers that can be reliably inhibited
- Leveraging our transcriptomic data and the Hyper-C in-silico platform, we constructed a computational astrocyte model with subsequent mechanistic analysis and drug target
- Our approach successfully recovers the approved drug Istradefylline for Parkinson Disease with clear mechanistic interference in astrocytes, counteracting the upregulated receptor ADORA2A.
- Utilizing this approach, potential novel drugs and drug combinations (Fillinger L et al., 2025) can be identified with clear mechanistic interference, counteracting disease phenotypes.







